Phonons, Isotope Effect, and Superconductivity in $Ba_{1-x}K_xBiO_3$: a Molecular Dynamics Simulation

Marcos H. Degani
Departamento de *Física* Geml e Aplicada Universidade *São* Francisco
Rua Alexandre Rodrigues Barbosa, 45, *13251-900,* Itatiba, SP, *Brazil*

Received **August 20,** 1994

The phonon density-of-states (DOS) of insulating $BaBiO_3$ in orthorhombic phase and superconducting $Ba_{1-x}K_xBiO_3$ in cubic phase are studied using the molecular dynamics (MD) method. The MD simulations are carried out with an effective interaction potential which includes Coulomb interactions, the charge-dipole interactions due to the electronic polarizability of O^{--}, and steric effects. Partial DOS of Ba, K, Bi and O in $BaBiO_3$ and $Ba_{1-x}K_xBiO_3$ are also determined from MD simulations and reveal that phonons above 20 meV are due to oxygen vibrations. The reference oxygen-isotope-effect exponent, $a_{,,} = -\partial \ln < w > / \partial \ln M_O$, of $Ba_{1-x}K_xBiO_3$ is determined to be $a_{,,} = 0.42 \pm 0.05$ from the mass (Mo) variation of the first moment of the phonon DOS, $^{16} < w >$ and $^{18} < w >$. This value is in very good agreement with the oxygen isotope-effect exponent α_0, determined experimentally from the variation of T_c, and suggests that $Ba_{1-x}K_xBiO_3$ is a weak-to-moderate coupling BCS-like superconductor and that the high T_c ($\approx 30K$) results from large electron-phonon matrix elements involving high-energy oxygen phonons.

I. Introduction

Since 1986 the physical mechanism responsible for high-temperature superconductivity in the oxide materials has been the focus of research in condensed matter physics[1]. In general, there are two kinds of oxide superconductors, one containing copper and the other without any transition metal elements[2]. Superconductivity in $Ba_{1-x}K_xBiO_3$ was first discovered by Mattheiss, Gyorgy, and Johnson[3] in 1988. The structure of the superconducting material was determined by Cava et al.[4] and a detailed account of synthesis, structure, and transition temperature as a function of x was given by Hinks et al.[5–7]. For x $\approx$ 0.4, $Ba_{1-x}K_xBiO_3$ exhibits superconductivity at $T_c \approx 30K$, which is the highest transition temperature reported for any oxide material not containing copper[2–16]. The superconducting phase of $Ba_{1-x}K_xBiO_3$ ($0.37 < x < 0.5$) forms a cubic perovskite cristal structure[17] which shows none of the planar structures observed in other high-T_c compounds. As the potassium concentration is reduced, superconductivity disappears when the structure changes from cubic to orthorhombic. Furthermore, $BaBiO_3$ is nonmagnetic[18,19] while the other high-T_c related material in the parent nonsuperconducting phases, display antiferromagnetism[20].

A wide range of experimental investigations have been carried out this system. According to neutron-diffraction measurements[17,21,22] potassium atoms are randomly distributed over the barium sites. Structural properties, electric, magnetic, thermal, and optical responses of the $Ba_{1-x}K_xBiO_3$ system have been studied. Raman-scattering[23], infrared-reflectivity[24,26], electron-tunneling[27–34], photoemission, and inverse photoemission[35,36], inelastic- neutron - diffraction[37–39], the oxygen isotope effect[8,18,40], specific heat[41–43] upper and lower critical magnetic fields[8,44–46], thermal conductivity[47], and thermoelectric power[18,48] have been measured. The crystalline structure and the phase diagram of $Ba_{1-x}K_xBiO_3$, as a function of temperature for the range x = 0 – 0.5 have been investigated by Pei et al.[17]. Hall effect measurements indicate that the carriers are electrons[18,49] whereas in the cuprates, with exception of $Nd_{2x}Ce_xCuO_4$ and $Pr_{2-x}Ce_xCuO_4$, the carriers are

holes[1].

Batlogg et al.[8] measured the oxygen isotope-effect by determining the shift in T_c between a 100% ^{16}O sample and a 65% ^{18}O exchanged sample of $Ba_{0.6}K_{0.4}BiO_3$ and they found an exponent $\alpha_0 = 0.22 \pm 0.03$ in the $T_c \sim M_O^{-\alpha_0}$ relation, where M_O is the mass of the oxygen isotope. Measurements by Hinks et al.[40] using a 100% ^{16}O and a 96% ^{18}O exchanged sample of $Ba_{0.625}K_{0.375}BiO_3$ indicate a substantial oxygen isotope effect, $\alpha_0 = 0.41 \pm 0.03$. Kondoh et al.[18] have determined $\alpha_0 = 0.35 \pm 0.05$. This value is larger than the isotope-effect exponents in high-T_c cuprate superconductors.

Attempts to carry out electron tunneling experiments in superconductor-insulator-superconductor (S-I-S) junctions in $YBa_2Cu_3O_{7-\delta}$ have not been very successful due to the very small coherence lenght ($\sim$ 10Å). In $Ba_{1-x}K_xBiO_3$, however, electron tunneling experiments on S-I-S junctions have recently been carried out by Zasadzinski et al.[27,28] and have revealed well- resolved structures in the high-energy range 30-60 meV in agreement with the phonon DOS obtained by neutron scattering experiments[37]. Sato et al.[31] have performed a tunneling experiments on thin films of $Ba_{0.6}K_{0.4}BiO_3$ and obtained the ratio $2\Delta(0)/K_BT_c = 3.7 \pm 0.5$, where A(0) is the superconducting energy gap at zero temperature, which is in agreement with the optically derived gap ratio by Schlesinger et

In this paper we report the calculation of the phonon densities of states of superconducting $Ba_{1-x}K_xBi^{16}O_3$ and $Ba_{1-x}K_xBi^{18}O_3$ (x = 0.4), and of insulating $BaBi^{16}O_3$. We find a significant softening of the oxygen phonon modes around 30 and 60 meV, in the superconducting material. In order to characterize the nature of superconductivity within the framework of BCS-Eliashberg theory[50,51] we investigate the correlation between the isotope shifts in the phonon DOS and in T_c of $Ba_{0.6}K_{0.4}Bi^{16}O_3$ and $Ba_{0.6}K_{0.4}Bi^{18}O_3$. We obtain a value of $a_{,,} = 0.42 \pm 0.05$ for $Ba_{0.6}K_{0.4}BiO_3$ which is very close to the isotope effect exponent in T_c. The results of our study indicate that $Ba_{1-x}K_xBiO_3$ is a weak-to-moderate coupling BCS superconductor, and the high superconducting transition temperature ($\sim$ 30K) results from large electron-phonon matrix elements involving high-energy oxygen modes. The superconducting properties of $Ba_{1-x}K_xBiO_3$ at zero and finite temperatures have been calculated within the framework of Eliashberg theory and compared with experiments by Jin, Degani, Kalia and Vashishta[52].

II. Molecular dynamics simulations of phonon density of states

The molecular dynamics method[53] was used to obtain the partial and total phonon densities of states. The MD simulations on $BaBiO_3$ were performed on a 540-particle system in the orthorhombic phase at the experimental density of 7.88 g/cm^3 with the lattice parameters a = 6.2000Å, b = 6.1561Å, and c = 8.6948Å, and 625 particles for $Ba_{0.6}K_{0.4}BiO_3$. In this system the substitution of 40% of the Ba atoms by K atoms was done randomly at the experimental density of 7.33 g/cm^3 in a cubic phase with lattice parameter a = 4.3160Å. The unit cells of the two systems are shown in Fig. 1. Effective interparticle interactions were used in the MD simulations. The Newton equations of motion are integrated by Beeman's method[54] using a time step of $\Delta t = 5 \times 10^{-15}$sec, which conserves energy to better than 1 part in 10^4 over several thousand time steps. The long-range nature of the Coulomb interaction is taken into account by Ewald's summation method[53].

In this simulation we have used effective pair-wise interactions. The potentials include charge-dipole interactions due to large electronic polarizability of O^{--} ions, steric repulsion between ions, and Coulomb interactions due to charge-transfer effects. The total potential has the form

$$V_{ij}(r) = (\alpha_i Z_j^2 + \alpha_j Z_i^2) e^{-r/r_{sc}}/2r^4 + H_{ij}/r^{\eta_{ij}} + Z_i Z_j/r\,, \quad (1)$$

where Z_i is the effective charge and α_i is the electronic polarizability of the ith ion and H_{ij} and η_{ij} are the strengths and exponents of the steric repulsion between the ions i and j, respectively. The screening length, $r_{,,}$ is chosen so that charge-dipole interaction does not have

a long tail. The steric repulsion balances the attractive interactions between cations and anions at short distances so as to give the correct bond lengths. The parameters for the interaction potentials, used in Eq. (1) for $BaBiO_3$ and $Ba_{0.6}K_{0.4}BiO_3$, are summarized in Tables I and II, respectively.

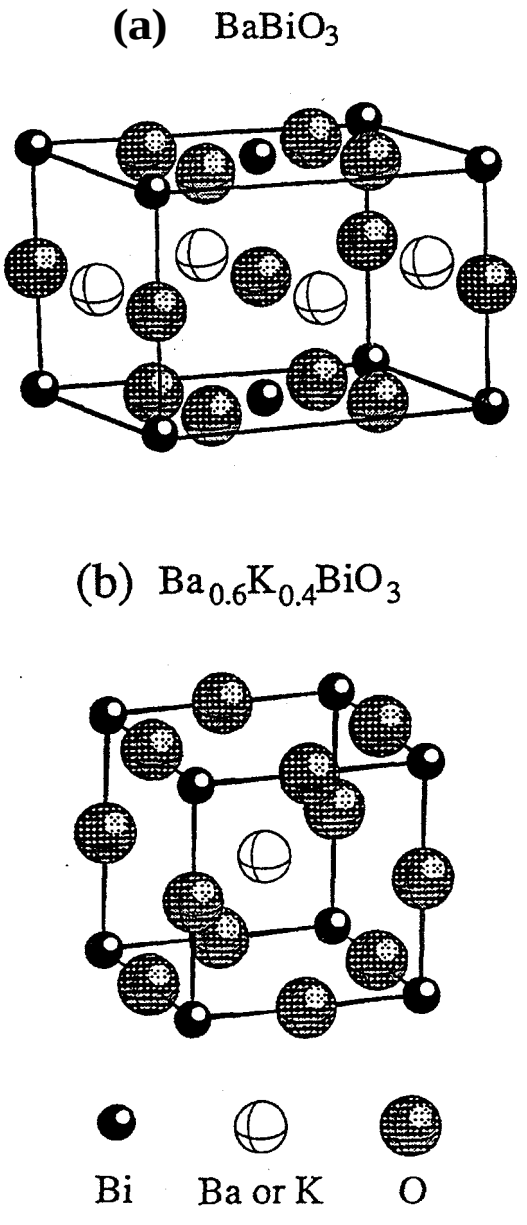

Figure 1: Crystal structures of (a) orthorhombic $BaBiO_3$ and (b) cubic $Ba_{0.6}K_{0.4}BiO_3$.

To establish the dynamical stability of the $BaBiO_3$, the system was put in the orthorhombic structure in an MD cell of fixed volume. The partial pair distribution functions and bond angle distribution functions were calculated to verify the bond lengths and coordi-

Table I - Constants in the effective potentials for $BaBiO_3$. Units of length and energy are Å and e^2/A = 14.39 eV respectively. Z is the effective charge (in units of $|e|$), a the electronic polarizability (A^3), η the repulsive exponent, and H the repulsive strength.

	Z	a
Ba	0.800	0.00
Bi	1.600	0.00
O	-0.800	2.40
r_{sc}	4.430	
	η	H
Ba-Ba	11	1186.8
Ba-Bi	11	157.3
Ba-O	9	281.5
Bi-Bi	11	13.2
Bi-O	9	60.8
O-O	7	49.2

Table II - Constants in the effective potentials for $Ba_{0.6}K_{0.3}BiO_3$. Units of length and energy are Å and $e^2/Å = 14.39$ eV respectively. Z is the effective charge (in units of $|e|$), a the electronic polarizability (A^3), η the repulsive exponent, and H the repulsive strength.

	Z	α
Ba	0.800	0.00
K	0.400	0.00
Bi	1.600	0.00
O	-0.747	2.40
r_{sc}	4.430	
	n	H
Ba-Ba	11	1007.0
Ba-K	11	1007.0
Ba-Bi	11	133.5
Ba-O	9	239.0
K-K	11	1007.0
K-Bi	11	133.5
K-O	9	239.0
Bi-Bi	11	11.2
Bi-O	9	51.6
O-O	7	41.8

nation numbers. The system was slowly heated to 600K and thermalized, for several thousand time steps. After this it was run uninterruptedly for more than 30,000 time steps and various structural correlations were calculated to examine the symmetry. The system at 600K was slowly cooled, thermalized, and then subjected to a steepest descent quench[55] (SDQ) which is a mathematically well defined method of examining the underlying mechanically stable structures. The partial pair correlation functions and bond angle distribution functions were calculated again to ascertain the symmetry of the MD system. After performing the above mentioned procedure on the $BaBiO_3$ system, it was determined that the resulting final symmetry was the same as that of the starting orthorhombic structure. The cubic $Ba_{0.6}K_{0.4}BiO_3$ system was also subjected to the same procedure to ensure dynamic stability.

The phonon density of states was calculated using two differents methods. We find that the results of all these two calculations are in agreement with one another. The first method involves calculating the velocity autocorrelation function for each species and the partial phonon DOS $F_i(\omega)$ is obtained by the Fourier transforms of this autocorrelation functions.

The normalized velocity-velocity autocorrelation function for βth species (β=Ba, Bi, K, or O) is given by

$$\Gamma_\beta(t) = \langle \sum_{i\in\{\beta\}} v_i(t)\cdot v_i(O)\rangle / \langle \sum_{i\in\{\beta\}} v_i(O)\cdot v_i(O)\rangle \ , \quad (2)$$

where v_i is the velocity of particle i and $< \ldots >$ is an average over MD configurations. The frequency spectrum of the $\Gamma_\beta(t)$ gives the partial phonon density of states

$$F_\beta(\omega)) = \int_0^\tau \Gamma_\beta(\omega t)\cos(\omega t) e^{-\gamma(t/\tau)^2} dt \ , \quad (3)$$

where a Gaussian window function with $\gamma = 1$ and $\tau = 3ps$ is used. The total density of states is obtained by summing the concentration weighted partial densities of states. Additional weighting with the coherent neutron cross-sections is required to obtain the neutron density of states.

The second method to calculate the phonon DOS involves the displacement autocorrelation function and the equation-of-motion method[53]. To implement this method it is essential to bring the system to a local minimum energy by carrying out the steepest descent quench which guarantees that the force and the velocity for each particle is zero. Each particle is then given a random displacement,

$$\delta_{ij}(O) = \delta_0 \cos(\theta_{ij}) \ , \quad (4)$$

where δ_0 is the amplitude of an initial displacement and θ_{ij} are random variables distributed uniformly between 0 and 2π. The system is allowed to evolve according to the classical equations of motion and the time variation of $r_{ij}(t)$is obtained. The displacement autocorrelation function is given by

$$f(t) = \sum_{ij} \delta r_{ij}(t)\delta r_{ij}(0) \ , \quad (5)$$

where $\delta r_{ij}(t) = r_{ij}(t) - r_{ij}(0)$. In the harmonic limit, the Fourier transforms of this autocorrelation functions give the density of states.

III. Results and discussion

To identify the physical origin of the peaks in the total DOS, we first examine the MD partial DOS for insulating $BaBiO_3$ and superconducting $Ba_{0.6}K_{0.4}BiO_3$. In Fig. 2, we show the MD partial DOS $F_{Ba}(\omega)$, $F_{Bi}(\omega)$, $F_O(\omega)$, and the total DOS $F(\omega)$ for $BaBiO_3$. The partial DOS is normalized to $3N_i$, where N, is the total particle number for the ith species in the MD system. It can be seen that all the peaks in $F_O(\omega)$ are located between 20 and 80 meV, $F_{Ba}(\omega)$ exhibits a single peak at 11 meV and $F_{Bi}(\omega)$ shows two peaks at 12 and 17 meV. Clearly, in the total DOS the peak at 11 meV is due to both Ba and Bi and the peak at 16 meV is due to Bi alone. Above 20 meV the entire spectrum arises from oxygen vibrations.

The MD results for the partial DOS, $F_{Ba}(\omega)$, $F_K(\omega)$, $F_{Bi}(\omega)$, $F_O(\omega)$ and the total DOS $F(\omega)$ for superconducting $Ba_{0.6}K_{0.4}BiO_3$ are presented in Fig. 3. Also in this system, all peaks located above 20 meV are due to oxygen vibrations. In contrast to $BaBiO_3$, $F_K(\omega)$ for $Ba_{0.6}K_{0.4}BiO_3$ shows an additional peak at 20 meV and the two-peak feature in $F_{Bi}(\omega)$ is

less pronounced. $F_O(\omega)$ of $BaBiO_3$ shows sharp peaks around 26, 32, 37, 40, 44, 51, 60, 66, and 74 meV. In $Ba_{0.6}K_{0.4}BiO_3$ the peaks between 20 to 40 meV merge into a band, and those between 60 and 80 meV broaden and show a slight shift to lower energies.

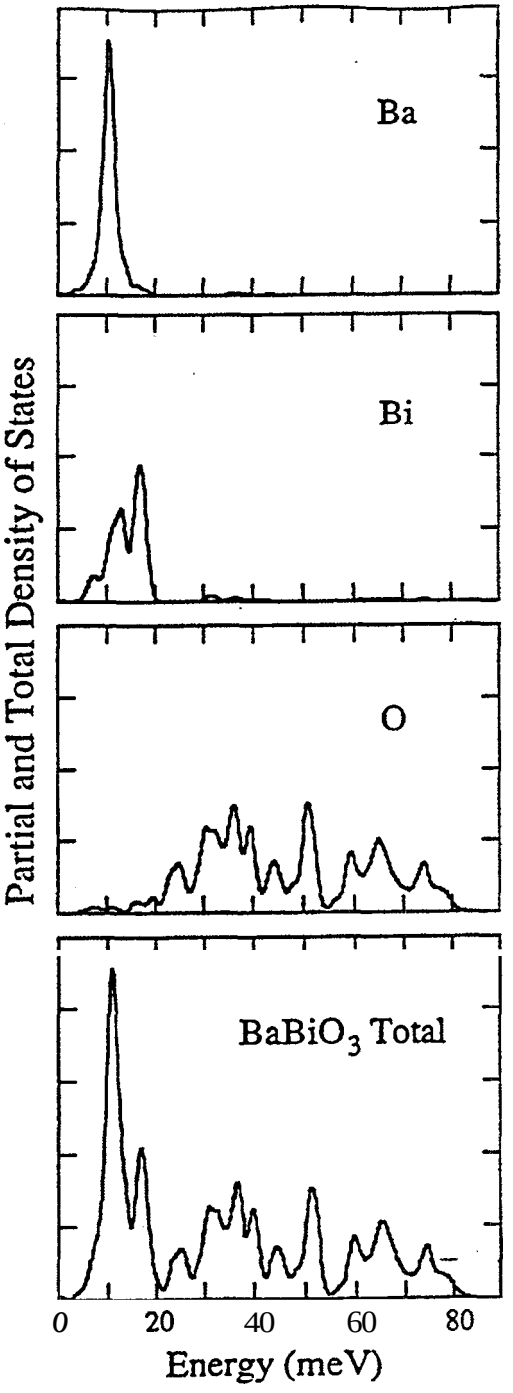

Figure 2: Molecular-dynamics results of partial and total phonon DOS for orthorhombic $BaBiO_3$.

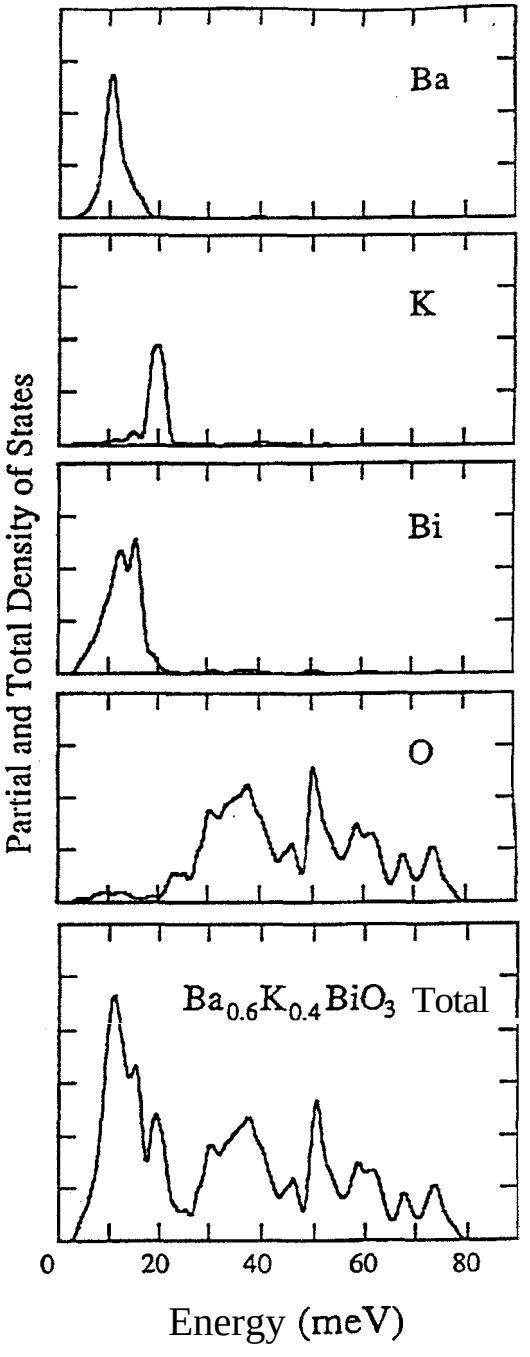

Figure 3: Molecular-dynamics results of partial and total phonon DOS for cubic $Ba_{0.6}K_{0.4}Bi^{16}O_3$.

In order to compare the neutron data[37] with MD simulation, we have calculated the neutron-weighted DOS, $G(\omega)$ using the partial DOS. The results are shown in Figs. 4 and 5 for $BaBiO_3$ and $Ba_{0.6}K_{0.4}BiO_3$, repectively. In general, there is an overall semiquantitative agreement between the MD results and neutron spectrum. In the case of $BaBiO_3$, the low-energy peaks at 11 and 17 meV cannot be resolved in the neutron data due to the relatively poor resolution in this

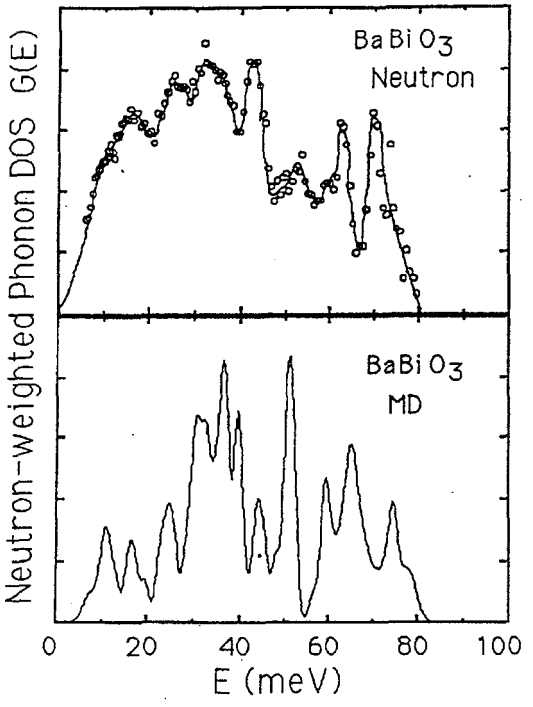

Figure 4: Neutron-weighted phonon DOS for $BaBiO_3$. Upper panel: INS experimental values (the solid line is a guide to the eye), and lower panel: molecular-dynamics simulation results.

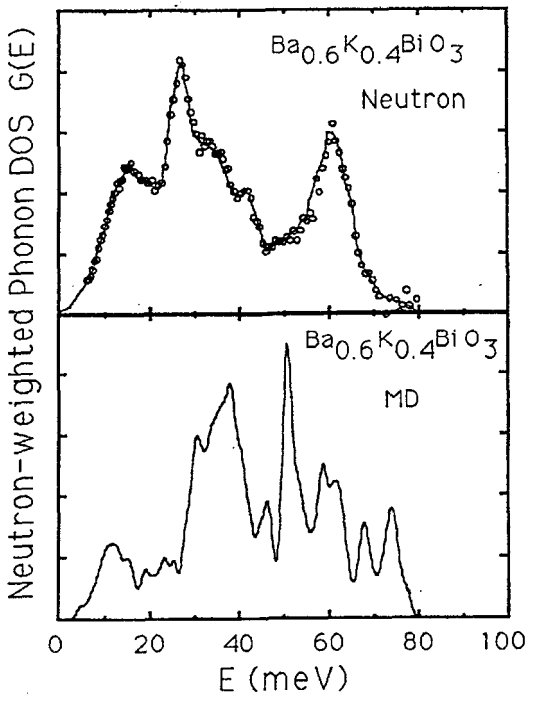

Figure 5: Neutron-weighted phonon DOS for $Ba_{0.6}K_{0.4}Bi^{16}O_3$. Upper panel: INS experimental values (the solid line is a guide to the eye), and lower panel: molecular-dynamics simulation results.

energy region. The difference between the MD and neutron $G(\omega)$ in the relative magnitude of the low-energy DOS is probably due to resolution effects and uncertainties of multiple-scattering background in the inelastic neutron scattering experiments. Otherwise, the peaks at 25, 30-40, 50, 60, and 65-75 meV of the MD DOS are identifiable with similar structures in the measured DOS. For $Ba_{0.6}K_{0.4}BiO_3$ the MD phonon DOS shows a three-band structure with intensities centered around 14, 35, and 65 meV. It is clear from INS measurements and MD simulation that the oxygen phonon modes soften by 5-10 meV with 40% K doping of $BaBiO_3$. Higher-resolution neutron measurements may reveal the additional features observed in the simulation.

IV. Isotope effect due to ^{16}O to ^{18}O substitution

The isotopic substitution of a particular atomic species will affect the superconducting transition temperature for a BCS superconductor as well as the phonon spectrum. The variation of T_c upon oxygen isotopic substitution is characterized by the oxygen isotope-effect exponent,

$$\alpha_0 = -\partial \ln T_c / \partial \ln M_O \ , \tag{6}$$

where M_O is the mass of the oxygen isotope.

When superconductivity is due to electron-phonon coupling and the strong coupling effects are included, the isotope effect of the lattice is reflected through the superconducting transition temperature,

$$T_c = \langle \omega \rangle e^{-f(\lambda,\ldots,\mu^*)} \ , \tag{7}$$

where $f(\lambda,\ldots,\mu^*)$ is an unknown functional determined from the solution of the Eliashberg gap equations without any weak-coupling approximation, λ is a dimensionless electron-phonon coupling constant, and μ^* is the Coulomb pseudopotential. The characteristic phonon frequency $< w >$ is defined as the first frequency moment,

$$< \omega >= \int \omega F(\omega) d\omega / \int F(\omega) d\omega \tag{8}$$

The oxygen isotope-effect exponent in Eq.(6) can be written as a sum of two terms obtained by differentiating Eq.(6):

$$\alpha_0 = \alpha_{or} - \delta\alpha_0 \tag{9}$$

where $a_{\prime\prime}$ is the reference isotope-effect exponent defined by

$$a_{\prime\prime} = -\partial \ln < \omega > / \partial \ln M_O \ . \qquad (10)$$

The reference isotope-effect exponent reflects the mass variation of the phonon DOS in a material whereas the oxygen mass variation of T_c is given by the isotope-effect exponent, α_0. $\delta\alpha_0$ is a measure of the contribution arising from the strong-coupling effects. Clearly, for a monoatomic weak-coupling superconductors α_0 is 1/2. In the presence of strong-coupling effects, α_0 will deviate from $a_{\prime\prime}$ due to a significant contribution from the factor $\exp[-f(\lambda, ..., \mu^*)]$. For multicomponent systems such as $Ba_{1-x}K_xBiO_3$, a partial isotope-effect exponent α_{ri} may be quite different[56] from 1/2 for isotopic substitution of the ith atomic species, e. g., ^{18}O for ^{16}O. A low value of α_0 does not necessarily mean that strong-coupling effects are important. A large $\delta\alpha_0$, on the other hand, implies that the strong-coupling effects are important.

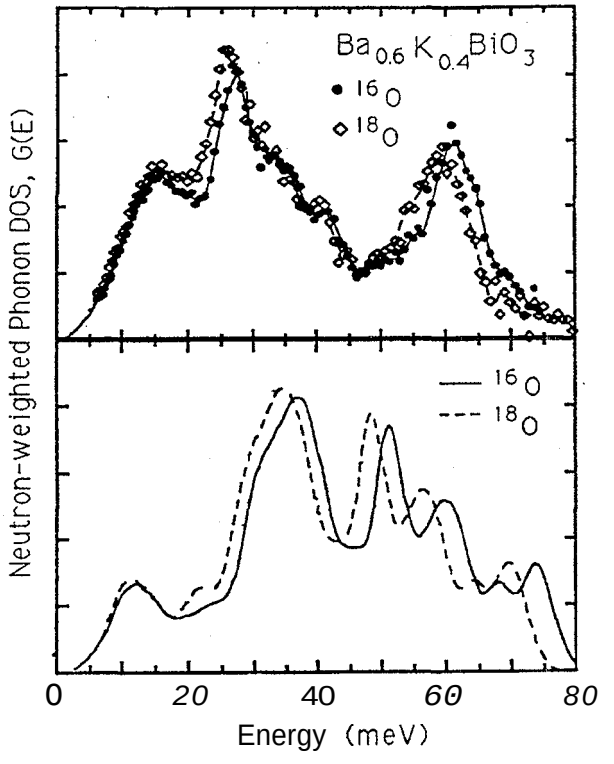

Figure 6: Neutron-weighted phonon DOS for $Ba_{0.6}K_{0.4}Bi^{16}O_3$ and $Ba_{0.6}K_{0.4}Bi^{18}O_3$. Upper panel: INS experimental values (the solid line is a guide to the eye), and lower panel: molecular-dynamics simulation results.

In Fig. 6 we show the neutron-weighted phonon DOS, G(E), for the ^{16}O and ^{18}O samples of $Ba_{0.6}K_{0.4}BiO_3$ obtained from INS and from MD simulations. The overall shape of the phonon DOS for the ^{18}O and ^{16}O is similar, except that above 20meV the phonon spectrum is shifted to lower energies by 3-4 meV. A similar behavior is observed from the MD results. The reference isotope-effect exponent α_{or} is found to be 0.42, which is in good agreement with the experimental values of a measured by Hinks et al.[40] (0.41 ± 0.03) and Kondoh et al.[18] (0.35 ± 0.05) from T_c, but significantly different from the results of Batlogg et al.[8] (0.22 ± 0.03).

V. Conclusion

In conclusion, this paper describes the MD simulations of isotopically substituted samples of an oxide superconductor. The comparison of the phonon DOS of the insulating $BaBiO_3$ with $Ba_{0.6}K_{0.4}BiO_3$ provides evidence for the importance of electron-phonon interaction in the superconducting $Ba_{1-x}K_xBiO_3$. The reference isotope-effect exponent of oxygen, $a_{\prime\prime}$, is estimated to be 0.42, only slightly higher than the isotope-effect exponent for T_c, $\alpha_0 = 0.41$. This result indicates that $Ba_{1-x}K_xBiO_3$ is a weak-to-moderate coupling BCS-like superconductor and the high T_c results from large electron-phonon matrix elements involving high-energy oxygen phonons.

Acknowledgments

I would like to thank my collaborators in this work, Dr. Chun-Keung Loong, Professor Priya Vashishta, Dr. Rajiv K. Kalia, and Dr. Wei Jin for valuable discussions. This work was partially supported by the Brazilian Agency CNPq.

References

1. J. C. Phillips, Physics of *High-T_c Superconductors* (Academic Press, San Diego, 1989); *High Temperature Superconductivity* - The Los Alamos *Symposium*, edited by K.S. Bedell, D. Coffey, D. E. Meltzer, D. Pines, and J. R. Schrieffer (Addison-Wesley, California, 1990).
2. I. K. Schuller and J. D. Jorgensen, MRS Bulletin, 14, No. 1, 27 (1989); J. D. Jorgensen and D. G. Hinks, Neutron News, **1,** No. 2, 24 (1991).

3. L. F. Mattheiss, E. M. Gyorgy and D. W. Johson, Jr., Phys. Rev. **B37**, 3745 (1988).
4. R. J. Cava, B. Batlogg, J. J. Krajewski, R. Farrow, L.W. Rupp Jr., A. E. White, K. Short, W. F. Peck and T. Kometani, Nature 332, 814 (1988).
5. D. G. Hinks, B. Dabrowski, J. D. Jorgensen, A. W. Mitchell, D. R. Richards, S. Pei and D. Shi, Nature 333, 836 (1988).
6. D. G. Hinks, D. R. Richards, B. Dabrowski, A. W. Mitchell, J. D. Jorgensen, D. T. Marx, Physica C 156, 477 (1988).
7. D. G. Hinks, A. W. Mitchell, Y. Zheng, D. R. Richards, B. Dabrowski, Appl. Phys. Lett. 54, 1585 (1989).
8. B. Batlogg, R. J. Cava, L. W. Rupp, Jr., A. M. Mujsce, J. J. Krajewski, J. P. Remeika, W. F. Peck, Jr., A. S. Cooper and G. P. Espinosa, Phys. Rev. Lett. 61, 1670 (1988).
9. L. F. Schneemeyer, J. K. Thomas, T. Siegrist, B. Batlogg, L. W. Murphy, Nature 335, 421 (1988).
10. R. J. Cava and B. Batlogg, MRS Bull, 14, 49 (1989).
11. B. Batlogg, in Mechanisms of High Temperature Superconductivity, edited by H. Kamimura and A. Oshiyama (Springer-Verlag, Berlim, 1989), p. 324.
12. B. Batlogg, R. J. Cava, L. F. Schneemeyer and G. P. Espinosa, IBM J. Res. Dev. 33, 208 (1989).
13. N. L. Jones, J. B. Parise, R. B. Flippen and A. W. Sleight, J. Solid State Chem. 78, 319 (1989).
14. S. Jin, T. H. Tiefel, R. C. Sherwood, A. P. Ramirez, E. M. Gyorgy, G. W. Kammlott and R. A. Fastnacht, Appl. Phys. Lett. 53, 1116 (1988).
15. S. Kondoh, M. Sera, K. Fukuda, Y. Ando and S. Sato, Solid State Commun. 67, 879 (1988).
16. T. J. Folkerts, R. N. Shelton and H. B. Radousky, Physica C 162-164, 550 (1989).
17. S. Pei, J. D. Jorgensen, B. Dabrowski, D. G. Hinks, D. R. Richards, A. W. Mitchell, J. M. Newsam, S. K. Sinha, D. Vaknin and A. J. Jacobson, Phys. Rev. **B41**, 4126 (1990).
18. S. Kondoh, M. Sera, Y. Ando and M. Sato, Physica C 157, 469 (1989).
19. Y. J. Uemura, B. J. Stemlieb, D. E. Cox, J. H. Brewer, R. Kadono, J. R. Kempton, R. F. Kieff, S. R. Kreitzman, G. M. Luke, P. Mulhern, T. Riseman, D. L. Willians, W. J. Kossler, X. H. Yu, C. E. Stronach, M. A. Subrarnanian, J. Gopalakrishnan and A. W. Sleight, Nature **335**, 151 (1988).
20. R. J. Birgeneau and G. Shirane, in Physical Properties of High Temperature Superconductors, edited by G. M. Ginsberg (World Scientific, Singapore, 1989), Vol. I, Chapter 4, and references therein.
21. S. Pei, J. D. Jorgensen, D. G. Hinks, B. Dabrowski, D. R. Richards, A. W. Mitchell, Y. Zheng, J. M. Newsam, S. K. Sinha, D. Vaknin and A. J. Jacobson, Physica C 162-164, 556 (1989).
22. S. Pei, J. D. Jorgensen, D. G. Hinks, B. Dabrowski, D. R. Richards, A. W. Mitchell, S. K. Sinha, D. Vaknin, J. M. Newsam and A. J. Jacobson, in Oxygen Disorder *Effects* in High-T_c Superconductors, edited by I. L. Moran-Lopez and I. K. Schuller (Plenum, New York, 1990), p. 1.
23. K. F. McCarty, H. B. Radousky, D. G. Hinks, Y. Zheng, A. W. Mitchell, T. J. Folkerts and R. N. Shelton, Phys. Rev. B40, 2662 (1989).
24. Z. Schlesinger, T. T. Colins, J. A. Calise, D. G. Hinks, A. W. Mitchell, Y. Zheng, B. Dabrowski, N. E. Bickers and D. J. Scalapino, Phys. Rev. **B40**, 6862 (1989).
25. R. T. Colins, Z. Schlesinger, F. Holtzberg, C. Feild, G. Koren, A. Gupta, D. G. Hinks, A. W. Mitchell, Y. Zheng and B. Dabrowski, in Strong Correlation and Superconductivity, edited by H. Fukuyama, S. Maekawa and A. P. Malozemoff (Springer-Verlag. Berlin, 1989), p.289.
26. Z. Schlesinger and R. T. Colins, MRS Bull. 15, 38 (1990).
27. J. F. Zasadzinski, N. Tralshawala, D. G. Hinks, B. Dabrowski, A. W. Mitchell and D. R. Richards, Physics **C158**, 519 (1989).
28. J. F. Zasadzinski, N. Tralshawala, J. Timpf, D. G. Hinks, B. Dabrowski, A. W. Mitchell and D. R. Richards, Physics C162-164, 1053 (1989).
29. Q. Huang, J. F. Zasadzinski, N. Tralshawala, K. E. Gray, D. G. Hinks, J. L. Peng and R. L. Greene, Nature 347, 369 (1990).
30. Q. Huang, J. F. Zasadzinski, K. E. Gray, D. R. Richards and D. G. Hinks, Appl. Phys. Lett. 57, 2356 (1990).
31. H. Sato, H. Takagi and S. Uchida, Physica **C169**,

391 (1990).

32. J. F. Zasadzinski, N. Tralshawala, Q. Huang, K. E. Gray and D. G. Hinks, IEEE Trans. Magn. **MAG-27,** 833 (1991).
33. F. Morales, R. Escudero, D. G. Hinks and Y. Zheng, Physics C169, 294 (1990); Physica B 169, 705 (1991).
34. F. Sharifi, A. Pargellis and R. C. Dynes, Phys. Rev. Lett. 67, 509 (1991).
35. T. J. Wagener, H. M. Meyer III, D. M. Hill, Y. Hu, M. B. Jost, J. H. Weaver, D. G. Hinks, B. Dabrowski and D. R. Richards, Phys. Rev. B40, 4532 (1989).
36. Y. Jeon, G. Liang, J. Chen, M. Croft, M. W. Ruckman, D. Di Marzio and M. S. Hegde, Phys. Rev. B41, 4066 (1990).
37. C. K. Loong, P. Vashishta, R. K. Kalia, M. H. Degani, D. L. Price, J. D. Jorgensen, D. G. Hinks, B. Dabrowski, A. W. Mitchell, D. R. Richards and Y. Zheng, Phys. Rev. Lett. 62, 2628 (1989).
38. C. K. Loong, D. G. Hinks, P. Vashishta, W. Jin, R. K. Kalia, M. H. Degani, D. L. Price, J. D. Jorgensen, B. Dabrowski, A. W. Mitchell, D. R. Richards and Y. Zheng, Phys. Rev. Lett. 66, 3217 (1991).
39. C. K. Loong, D. G. Hinks, W. Jin, M. H. Degani, D. L. Price, J. D. Jorgensen, B. Dabrowslti, A. W. Mitchell, D. R. Richards, Y. Zheng, P. Vashishta and R. K. Kalia, in Electron-Phonon Interaction in Oxide Superconductors, edited by J. P. Carbotte and R. Baquero (World Scientific, Singapore, 1991).
40. D. G. Hinks, D. R. Richards, B. Dabrowski, D. T. Marx,and A. W. Mitchell, Nature 335,419 (1988).
41. S. E. Stupp, M. E. Reeves, D. M. Ginsberg, D. G. Hinks, B. Dabrowski and K. G. Vandervoort, Phys. Rev. B40, 10878 (1989).
42. M. F. Hundley, J. D. Thompson and G. H. Kwei, Solid State Commun. 70, 1155 (1989).
43. J. E. Graebner, L. F. Schneemeyer and J. K. Thomas, Phys. Rev. B39, 9682 (1989).
44. W. K. Kwok, U. Welp, G. W. Grabtree, K. G. Vandervoot, R. Hulscher, Y. Zheng, B. Dabrowski and D. G. Hinks, Phys. Rev. B40, 9400 (1989).
45. U. Welp, W. K. Kwok, G. W. Grabtree, H. Claus,K. G. Vandervoort, B. Dabrowski, A. W. Mitchell, D. R. Richards, D. T. Marx and D. G. Hinks, Physics C156, 27 (1988).
46. G. W. Grabtree, W. K. Kwok, U. Welp, K. G. Vandervoort, B. Dabrowski and D. G. Hinks, Physica B 163, 652 (1990).
47. S. D. Peacor, R. A. Richardson, J. Burrn, C. Uher and A. B. Kaiser, Phys. Rev. B42, 2684 (1990).
48. M. Sera, S. Kondoh and M. Sato, Solid State Commun. 68, 647 (1988).
49. H. Sato, S. Tajima, H. Takagi and S. Uchida, Nature 338, 241 (1989).
50. J. R. Schrieffer, Theory *of* Superconductivity (Benjamin, New York, 1964).
51. D. J. Scalapino, in Saperconductivity, edited by R. D. Parks (Dekker, New York, 1969), Vol. I, p. 449.
52. W. Jin, M. H. Degani, R. K. Kalia and P. Vashishta, Phys. Rev. B45, 5535 (1992).
53. A. Rahman and P. Vashishta, in Physics of *Su*perionic Coonductors, edited by J. W. Perram (Plenum, New York, 1983), p.93.
54. D. Beeman and R. Alben, Adv. Phys.26, 339 (1977).
55. R. Fletcher, *Pratical* Methods of Optimization (Wiley, New York, 1980), and F. H. Stillinger and T. A. Weber, Science 225, 983 (1984).
56. J. P. Carbotte, in Electron-Phonon Interaction *in* Oxide Superconductors, edited by J. P. Carbotte and R. Baquero (World Scientific, Singapore, to be published).